Comptes Rendus

Chimie

Amélie Bordage, Adama N'Diaye and Anne Bleuzen

Prussian Blue analogs and transition metal K-edge XMCD: a longstanding friendship

Review / *Revue*

Prussian Blue analogs and transition metal K-edge XMCD: a longstanding friendship

Amélie Bordage *, a, **Adama N'Diaye**[a] and **Anne Bleuzen** [a]

[a] ICMMO, Université Paris-Saclay, CNRS, Orsay, France

E-mails: amelie.bordage@universite-paris-saclay.fr (A. Bordage),
adama.ndiaye@universite-paris-saclay.fr (A. N'Diaye),
anne.bleuzen@universite-paris-saclay.fr (A. Bleuzen)

Abstract. Prussian Blue analogs (PBAs) are well-known coordination polymers offering a wide range of properties, and their fundamental understanding requires their investigations by various techniques. One of them is transition metal (TM) K-edge X-ray Magnetic Circular Dichroism (XMCD), which is element selective, bulk sensitive and compatible with a wide range of experimental conditions. This short review presents the reciprocal investigation of PBA with TM K-edge XMCD, from the first studies demonstrating that qualitative local magnetic information could be obtained on PBA from TM K-edge XMCD until our on-going project aiming at fundamentally understanding TM K-edge XMCD thanks to PBAs as model-compounds.

1. Introduction

Prussian Blue ($Fe_4^{III}[Fe^{II}(CN)_6]_3 \cdot xH_2O$) was discovered at the beginning of the 18th century [1,2] and is considered as the very first synthetic coordination polymer, first mainly used in pigments for paintings [3]. This fortuitous discovery opened a new branch in chemistry dedicated to the investigation of Prussian Blue Analogs (PBAs), which are obtained by replacing the Fe ions by other transition metals (TM). They are now synthesized as powders (whose grains are generally comprised between few nanometers and some hundreds of nanometers), nanoparticles and molecular-derivatives, and used/investigated as precursors of oxides and alloys and functional materials for data storage, medical applications, catalysis, batteries, sensors,... [4–23]. For the fundamental study of their properties, the chemist usually takes advantage of all the state-of-the-art analytical techniques available, with contributions from experiments and theory.

For the last 30 years, synchrotron-based spectroscopic techniques have proven to be priceless for the study of PBAs and their derivatives. In particular, X-ray Absorption Spectroscopy (XAS) has significantly contributed to the enrichment of the PBA knowledge, especially because XAS is a chemically selective technique and hence can individually probe each transition metal of the PBA, which most of the time belongs to the first row transition metals. Given its orbital selectivity, XAS can also probe different empty orbitals (the 3*d* ones for the TM $L_{2,3}$-edges

---

and the $4p$ ones for the TM K-edge), and thus gives access to different structural and electronic information. XAS is mainly used to determine the oxidation and/or spin states and the local structure of the transition metals of the PBAs [24–30]. Another advantage of XAS is that the measurements can be performed *in situ*, for instance at 4K under photoexcitation, which made it a valuable probe of thermally- or photoinduced electron transfers [31–38]. Another example of the interest of XAS for PBA is the recent evidence of a core–shell structure of CoFe PBAs nanoparticles confined within the porosity of a silica monolith [39]. Using a crystal-analyzer spectrometer to perform High Energy-Resolution Fluorescence-Detected (HERFD) XAS [40], individual information on each species of Fe ions in the native Prussian Blue could also be obtained [41].

As a derivative technique from XAS, X-ray Magnetic Circular Dichroism (XMCD) has also been applied to PBAs. At the TM $L_{2,3}$-edges [42], the magnetic $3d$ orbitals are directly probed, making XMCD a direct probe of the individual magnetic properties of each transition metal of the PBA, with the possibility to extract quantitative information about the spin and orbital momenta thanks to the sum rules [43,44] and/or multiplet calculations [45]. The energy of the incident X-ray requires ultra-high vacuum and enables to probe only a few nanometers of the sample. Therefore, TM $L_{2,3}$-edges XMCD was mainly applied to the study of thin films, nanoparticles and molecular-derivatives [8,22,46–49]. It can also provide information on bulk compounds, but only on their surface [50]. On the contrary, TM K-edge XMCD [51–54] lies in the hard X-ray regime and so (i) allows for experiments with demanding sample environments, for instance high-pressure [55,56], and (ii) probes all the species of the absorbing atom. It however probes the delocalized $4p$ orbitals, which *a priori* prevents from getting direct magnetic information but could offer the possibility to get fine structural information. The theoretical framework of TM K-edge XMCD is also less established than for the $L_{2,3}$-edges, despite the several attempts made to understand and disentangle the physical effects at the origin of these signals [57–63].

We present here a short review on how PBAs and TM K-edge XMCD reciprocally generate information on each other. We summarize the main results obtained on PBAs and TM K-edge XMCD since the very first investigations of the exchange interaction in PBA using TM K-edge XMCD performed by Michel Verdaguer and his team in the 90's until our on-going project aiming at disentangling the physical effects at the origin of TM K-edge XMCD signals and quantifying small structural distortions from these signals using PBA as model compounds to finally make it a real tool for chemists. During the first 20 years, only qualitative relationships could be established between a feature of the XMCD signal and a property of the PBA: the sign to some magnetic properties (Section 2) and the intensity to the structure (Section 3). This however proved that TM K-edge XMCD can offer priceless opportunities for the investigation of the PBA properties and must therefore be fully understood, a task our group is now addressing (Section 4).

2. The very first investigations: the nature of the exchange interaction

The very first adventures of PBA with XMCD started in the general context of finding molecule-based magnets with a Curie temperature above room-temperature. Verdaguer and co-workers concentrated their work on the PBA family [64–67]. To better understand the magnetic coupling between the two TMs in their high-T_C magnets CsMn[Cr(CN)$_6$], CsNi[Cr(CN)$_6$] and Ni$_3$[Cr(CN)$_6$]$_2$, they recorded the XMCD signals at the K-edge of each transition metal (Cr, Mn, Ni) [67–69]. In the CsNi[Cr(CN)$_6$] PBA, known to present a ferromagnetic coupling between the Ni^{2+} and Cr^{3+} ions, they observed (i) a derivative-shape signal at the Cr K-edge with a negative first lobe and a positive second one, and (ii) a positive single-peak signal at the Ni K-edge. In CsMn[Cr(CN)$_6$], known to present a antiferromagnetic coupling between the Mn^{2+} and Cr^{3+} ions, the signal at both K-edges has a derivative shape but of opposite signs between the Mn and Cr K-edges. They concluded that the relative sign of the XMCD signals at the two TM K-edges gives the magnetic coupling between these TMs. They could also identify the TM carrying the larger magnetic moment.

Shortly after this pioneering work, they used this new knowledge on TM K-edge XMCD to characterize two new room-temperature ferrimagnets, $V^{II}_{0.45}V^{III}_{0.53}[V^{IV}O]_{0.02}[Cr^{III}(CN)_6]_{0.69}$ (called **VCr**) and $Cs^I_{0.82}V^{II}_{0.66}[V^{IV}O]_{0.34}[Cr^{III}(CN)_6]_{0.92}$ (called **CsVCr**) [4,69,70]. They could first confirm the nature of the

exchange interaction between the V and Cr ions: both PBAs present an antiferromagnetic coupling. But the main result comes from the local magnetic information now accessible by TM K-edge XMCD thanks to their previous observation for $CsMn[Cr(CN)_6]$ and $CsNi[Cr(CN)_6]$. For **VCr**, a positive/negative signal is observed at the Cr K-edge and a negative/positive one at the V K-edge, meaning, within their sign convention, that the V^{2+} ions carry the larger magnetic moments. On the contrary, the negative/positive signal is observed at the Cr K-edge for **CsVCr** (Figure 1a), meaning that the Cr^{3+} ions carry the larger magnetic moments. This opposite sign of the Cr K-edge signal between **VCr** and **CsVCr** is a clear experimental evidence of the reversal of the local magnetization on V and Cr with the change of stoichiometry, despite an identical nature of the exchange interaction [4,69].

In parallel to their search of high-T_C magnets, Verdaguer and co-workers also undertook a study of CoFe PBAs [27,28,32,72,73], among them the $Rb_{1.8}Co_4[Fe(CN)_6]_{3.3}$ PBA (called **Rb₂CoFe**) which presents a $Co^{III}Fe^{II} \rightarrow Co^{II}Fe^{III}$ photoinduced reversible charge-transfer at low temperatures [27,32]. The original work by Hashimoto on photomagnetic CoFe PBAs [74] indeed launched a series of studies on photomagnetic PBAs in order to fully understand the phenomenon. In the case of **Rb₂CoFe**, since a macroscopic characterization of the photoinduced metastable state by SQUID magnetometry was not feasible, Verdaguer and his team turned to Fe and Co K-edges XMCD to elucidate the nature of the exchange interaction between the Fe^{3+} and Co^{2+} ions [5,71,72]. They recorded the signals in the photoinduced state for **Rb₂CoFe** and for the $Co_4[Fe(CN)_6]_{2.7}$ PBA (called **CoFe**) in its ground state as a reference (Figure 1b), since in this compound the exchange interaction is known to be antiferromagnetic [75]. For both compounds and at both edges, the signal consists in a single main contribution. The key point is that the sign of the signals is opposite between the Fe and Co edges, meaning that the exchange interaction between the Fe^{3+} and Co^{2+} ions is antiferromagnetic. For **CoFe**, this is consistent with the macroscopic magnetic data. For **Rb₂CoFe** in its photoexcited state, that was the first experimental evidence of the ferrimagnetic nature of its photoexcited state [71].
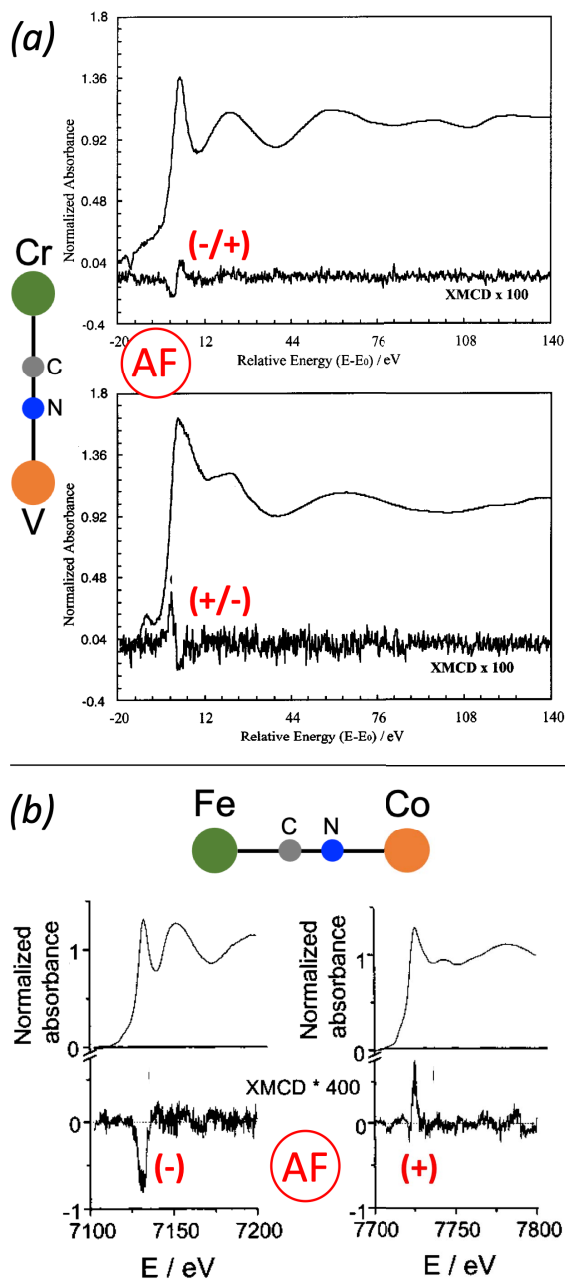
Figure 1. (a) Cr (up) and V (down) K-edges XMCD signals and XANES spectra of **CsVCr**. (b) Fe (left) and Co (right) K-edges XMCD signals and XANES spectra of **CoFe**. Adapted from Refs [69] and [71].

More recently, Lahiri and co-workers used Fe and Mn K-edge XMCD to identify the origin of the magnetic-field actuated magnetization polarity

reversal in the $Cu_{0.73}Mn_{0.77}[Fe(CN)_6]$ PBA they observed by SQUID magnetometry [76]. They recorded for each edge the XMCD signal for an external magnetic field of 0.02 T and 2 T. The sign of the Fe K-edge XMCD signal does not change with the external magnetic field, but the Mn K-edge signal reverses its sign when changing the strength of the applied magnetic field. They could thus propose that the field actuated magnetization crossover arises from a Mn spin flip.

3. Going further: XMCD as a potential structural probe

Several years later, motivated by better understanding the structure-property relationship in PBAs, Bleuzen and co-workers thought about TM K-edge XMCD as a potential new probe to characterize the slight structural distortions of the A–NC–B linkage that seemed to be the key-parameter to control and modulate several properties of PBAs. TM K-edge indeed probes the empty $4p$ orbitals, which are delocalized and so *a priori* sensitive to slight structural distortions. They investigated on the ODE beamline [56,77] at SOLEIL synchrotron (France) a series of four NiFe PBAs ($Y_xNi_4[Fe(CN)_6]_{(8+x)/3}$, with $x = 0, 1, 2$ for Y = Cs and $x = 2$ for Y = Rb) under pressure (between 0 and 7 GPa) by Fe and Ni K-edge XMCD [78,79]. These PBAs were chosen since they present no piezo-induced charge-transfer, which allowed to relate any changes observed in XMCD only to structural events. A summary of the study is presented below and illustrated in Figure 2.

Whatever the induced pressure, the Fe K-edge signals present the same number of features at the same energy; the same observation stands at the Ni K-edge. Nevertheless, the intensity is almost doubled between 0 and 0.8 GPa, and then decreases until it completely disappears. The intensity of TM K-edge XMCD is highly sensitive to slight structural distortions. This complex pressure-dependent behavior of the intensity is observed for the four PBAs but cannot be explained solely by a simple compression of the unit cell. The evolution of both the XMCD signals and the X-ray absorption spectra shows a pressure-induced structural change of the Ni^{2+} coordination polyhedra that the authors proposed to explain by a progressive tilt of the Ni^{2+} ions around their crystallographic position and/or of the $[Fe(CN)_6]$ rigid

unit around the Fe^{3+} ions crystallographic position when pressure is applied. A second interesting point is that the disappearance of the signal at the Fe and Ni K-edges occurs at different pressures. This asymmetric behavior of the Ni^{2+} and Fe^{3+} ions means that the local symmetry and its evolution with pressure are different for each TM. Additionally, it means that independent information on each TM of the PBA can be obtained. Finally, they showed through the quantitative analysis of the signals at each edge that the Ni^{2+} ions contribute to the Fe K-edge XMCD signal, while the Fe^{3+} ions do not contribute to the Ni K-edge signal.

The authors could propose an explanation for all their observations in terms of $3d$–$4p$ and $4p$–$4p$ orbitals overlap and local symmetry of the TMs, which is illustrated for each edge in the right schemes of Figure 2. It must first be noted that the coupling of XMCD with SQUID magnetometry established that the XMCD intensity changes observed with pressure cannot be attributed to a change in the $3d$–$3d$ inter-sites exchange interactions (J_{Ni-Fe}^{3d-3d}). Then, the identical contribution of the Ni^{2+} ions to the Ni and Fe K-edges implies that the exchange interaction between the photoelectron in the $4p$ orbital and the unpaired Ni $3d$ electrons is delocalized, the $4p$ electronic structure being described by the mixing of the two $4p_{Ni}$ and $4p_{Fe}$ mixed sub-bands. The third involved effect is the exchange interaction between the photoelectron in the delocalized $4p$ states and the unpaired electrons in the $3d$ orbitals, which is composed of the direct exchange interaction (present whatever the edge) and orbitals mixing (depending on the local symmetry of the TM). This contribution of the orbitals mixing accounts for the non-reciprocal contribution of the Ni^{2+} ions to the Fe K-edge signal: at the Ni K-edge, the Ni coordination polyhedron is not centrosymmetric, leading to a $3d_{Ni}$–$4p_{Ni}$ orbital mixing, while the octahedral $[Fe(CN)_6]$ units prevents $3d_{Fe}$–$4p_{Fe}$ orbital mixing.

4. Towards a full understanding of TM K-edge XMCD

The first studies [4,5,67–72] hence introduced TM K-edge XMCD as a powerful tool to get local magnetic information on coordination polymers, either to directly confirm macroscopic measurements or to study states inaccessible by other techniques. The
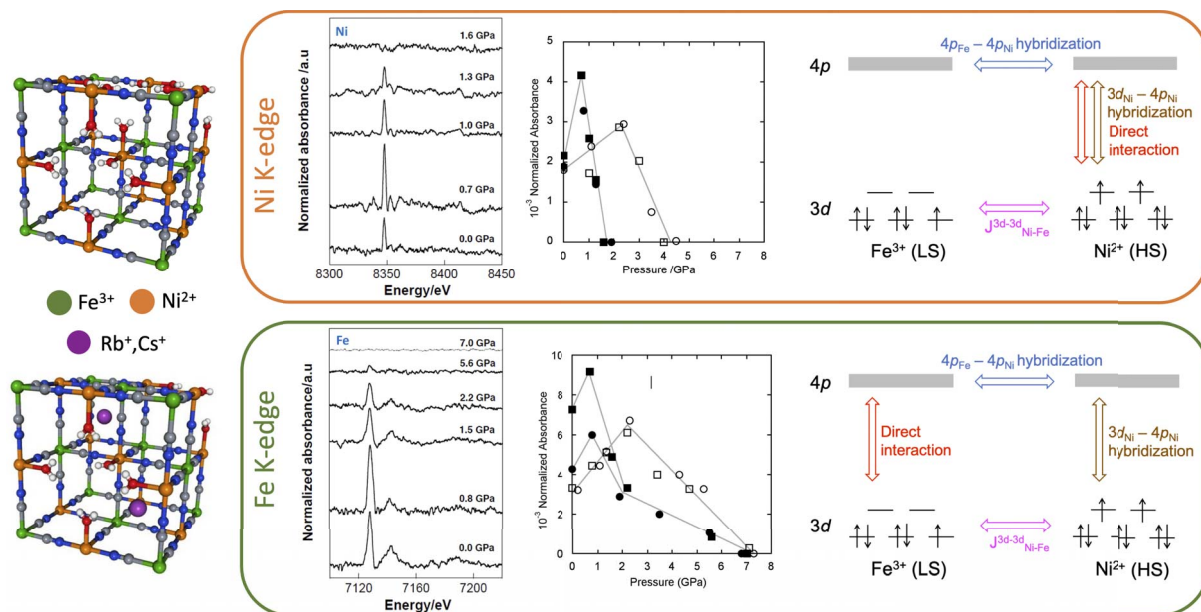
Figure 2. Scheme of the unit cell for the $Ni_4[Fe(CN)_6]_{2.7}$ PBA and the $Y_2Ni_4[Fe(CN)_6]_{3.3}$ PBA. Variable pressure XMCD signals of $Ni_4[Fe(CN)_6]_{2.7}$, variation of the XMCD intensity with pressure for the four PBAs ($Ni_4[Fe(CN)_6]_{2.7}$ = black squares, $Cs_1Ni_4[Fe(CN)_6]_3$ = black circles, $Cs_2Ni_4[Fe(CN)_6]_{3.3}$ = white squares and $Rb_2Ni_4[Fe(CN)_6]_{3.3}$ = white circles) and scheme of the orbitals and interactions contributing to the signal at the Ni K-edge (upper panel) and at the Fe K-edge (lower panel). Adapted from Ref. [78].

relative sign of the XMCD signal at the two edges of the TMs of the PBA is established as a clear and unambiguous signature of the nature of the exchange interaction between the two metallic ions. It also enables to identify the metallic ion carrying the larger magnetic moment. However, despite numerous efforts, this information then remained the only ones accessible by TM K-edge XMCD, which highly limited its rise among the chemists' community. Then, several years after, a quite isolated study showed that the intensity of TM K-edge XMCD is related to structural changes, but again only in a qualitative way [78,79]. These results constituted the first step towards the disentanglement of the localized and delocalized components of the TM K-edge XMCD signal. They also importantly established that the TMs in a PBA display an independent behavior, which is critical to disentangle the physical effects at the origin of TM K-edge XMCD and so proves that the PBAs are well-suited model compounds to tackle this longstanding question. Therefore, to finally make TM K-edge XMCD a usable magnetic and structural local probe for the chemists' community, we have undertaken

a rigorous step-by-step investigation of TM K-edge XMCD using PBAs as model compounds.

We first addressed the effects of the external parameters on the XMCD signal [80,81]. A true understanding of the physical effects at the origin of TM K-edge XMCD can indeed be gained only if any change observed in the XMCD signal can be unambiguously attributed to a change in the internal parameter of the PBA model compounds under consideration, without a doubt about the data treatment or the experimental conditions used to record the TM K-edge XMCD signals. The two $Ni_4[Fe(CN)_6]_{2.7}$ (called **NiFe**) and **CoFe** PBAs were investigated in detail to understand the effects of temperature and magnetic field. Below the magnetic ordering temperature, neither the number nor the energy of the spectral features are affected by them, unlike the intensity which increases as temperature or magnetic field increase, the temperature being the most critical parameter. Calculations also demonstrated that for the ODE beamline, where all our XMCD experiments are carried out, the circular polarization rate is constant on the energy range of the TM K-edges. Finally, an

optimized data treatment procedure was defined. This preliminary but critical study enabled to define an XMCD measurement and data treatment procedure to trustfully investigate the effect of selected changes in internal PBA parameters. More generally, we could also propose guidelines to perform reliable TM K-edge XMCD experiments on molecular compounds.

The next steps of this project are:

- disentangling the physical effects at the origin of TM K-edge XMCD thanks to well-chosen series of model PBAs,
- relating changes in the XMCD signal to electronic and structural features of the model PBAs,
- developing a methodology to quantify the slight structural distortions of the A–NC–B linkage of the PBA from TM K-edge XMCD.

For these steps, the model PBAs all derive from the **NiFe** reference of the pressure-dependent study [78]. We built series of reference PBAs by independently varying chemical, structural and electronic parameters. These series are experimentally investigated by coupling the characterizations of their properties at the macroscopic and local scales [81].

5. Conclusion and perspectives

All these studies of PBAs by TM K-edge XMCD showed the potential opportunities of this spectroscopic tool, despite the lack of a well-established theoretical framework and of fundamental understanding of this spectroscopy. Its development for PBAs was not straightforward, especially since very few groups endeavored to fundamentally understand the physical processes at the origin of the signals and make TM K-edge XMCD accessible and a routine technique for the investigation of PBA and other molecular compounds. Almost 30 years have passed since the first qualitative interpretation for the determination of the nature of the exchange coupling between the two TM ions [68] to first promising results [80,81] that will undoubtedly lead to unambiguous clear relationship between the magnetic behavior of the probed TM and the spectral features of TM K-edge XMCD.

Thanks to this current understanding of TM K-edge XMCD for coordination polymers, challenging and stimulating perspectives in the study of coordination polymers, nanoparticules [18,39] or molecular derivatives [10,14,16,21,22] await chemists. These future investigations will also benefit from ongoing experimental and theoretical developments. Almost all synchrotrons in the world are evolving towards 4th generation ring, which will improve their performance and open new possibilities for experimental developments, especially since the improvement of the machine itself and hence of the delivered X-ray beam (brilliance, reduced size, coherence...) is accompanied by developments of detectors, experimental setups and a general upgrade of beamlines. For instance, thanks to higher flux and improved stability, RIXS-XMCD [82–85] at the $3d$ TM K pre-edges may for instance become much more accessible. This photon-in photon-out spectroscopy has the main drawback to be very photon-hungry, but it offers the possibility to probe the same final states as in TM $L_{2,3}$-edges with hard X-ray when performed in the 3d TM K pre-edge region [83]. Combined with Ligand Field Multiplet calculations and TM K-edge XMCD recorded in the classical total fluorescence yield mode [86], it can bring very fine information on the absorbing atom (for instance on the spin-orbit coupling, the Coulomb repulsion...). RIXS-XMCD can also bring site-selective information, as it was demonstrated for magnetite [82], or complex samples such as core–shell nanoparticle [84,85]. The last envisioned development of TM K-edge XMCD for PBAs is fully theoretical, with the calculation of the TM K-edge XMCD signal, which could help to finalize the disentanglement of the physical processes at the origin of these signals. Advances in these calculations were indeed recently made thanks to a first-principles semi-relativistic approach which relies on density functional theory with plane waves and pseudopotentials [62,87], approach which showed a good agreement between experiments and theory for several ferromagnetic metals [62] and iron hydride under pressure [63].

Conflicts of interest

Authors have no conflict of interest to declare.

Acknowledgment

References

[1] A. Kraft, *Bull. Hist. Chem.*, 2008, **33**, 61-67.

[2] J. Brown, *Phil. Trans.*, 1724, **33**, 17-24.

[3] J. Bartoll, "The early use of Prussian Blue in paintings", in *9th International Conference on NDT of Art 2008* (Jerusalem, Israel), 2008.

[4] M. Verdaguer, A. Bleuzen, V. Marvaud, J. Vaissermann, M. Seuleiman, C. Desplanches, A. Sciuller, C. Train, R. Garde, G. Gelly, C. Lomenech, I. Rosenman, P. Veillet, C. Cartier, F. Villain, *Coord. Chem. Rev.*, 1999, **190–192**, 1023-1047.

[5] A. Bleuzen, V. Marvaud, C. Mathonière, B. Sieklucka, M. Verdaguer, *Inorg. Chem.*, 2009, **48**, 3453-3466.

[6] S. Lepoutre, D. Grosso, C. Sanchez, G. Fornasieri, E. Rivière, A. Bleuzen, *Adv. Mater.*, 2010, **22**, 3992-3996.

[7] D. M. Pajerowski, J. E. Gardner, D. R. Talham, M. W. Meisel, *New J. Chem.*, 2011, **35**, 1320-1326.

[8] D. M. Pajerowski, J. E. Gardner, F. A. Frye, M. J. Andrus, M. F. Dumont, E. S. Knowles, M. W. Meisel, D. R. Talham, *Chem. Mater.*, 2011, **23**, 3045-3053.

[9] L. Hu, J.-Y. Mei, Q.-W. Chen, P. Zhang, N. Yan, *Nanoscale*, 2011, **3**, 4270-4274.

[10] N. Dia, L. Lisnard, Y. Prado, A. Gloter, O. Stéphan, F. Brisset, H. Hafez, Z. Saad, C. Mathonière, L. Catala, T. Mallah, *Inorg. Chem.*, 2013, **52**, 10264-10274.

[11] R. Jeon, S. Calancea, A. Panja, D. M. Pinero Cruz, E. S. Koumousi, P. Dechambenoit, C. Coulon, A. Wattiaux, P. Rosa, C. Mathonière, R. Clérac, *Chem. Sci.*, 2013, **4**, 2463-2470.

[12] L. Guadagnini, M. Giorgetti, D. Tonellu, *J. Solid State Electrochem.*, 2013, **17**, 2805-2814.

[13] O. N. Risset, P. A. Quintero, T. V. Brinzari, M. J. Andrus, M. W. Lufaso, M. W. Meisel, D. R. Talham, *J. Am. Chem. Soc.*, 2014, **136**, 15660-15669.

[14] E. S. Koumousi, I.-R. Jeon, Q. Gao, P. Dechambenoit, D. N. Woodruff, P. Merzeau, L. Buisson, X. Jia, D. Li, F. Volatron, C. Mathonière, R. Clérac, *J. Am. Chem. Soc.*, 2014, **136**, 15461-15464.

[15] M. Giorgetti, D. Tonelli, M. Berrettoni, G. Aquilanti, M. Minicucci, *J. Solid State Electrochem.*, 2014, **18**, 965-973.

[16] D. Aguilà, Y. Prado, E. Koumousi, C. Mathonière, R. Clérac, *Chem. Soc. Rev.*, 2016, **45**, 203-224.

[17] V. Trannoy, M. Faustini, D. Grosso, F. Brisset, P. Beaunier, E. Rivière, M. Putero, A. Bleuzen, *Nanoscale*, 2017, **9**, 5234-5243.

[18] L. Catala, T. Mallah, *Coord. Chem. Rev.*, 2017, **346**, 32-61.

[19] F. Ma, Q. Li, T. Wang, H. Zhnag, G. Wu, *Sci. Bull.*, 2017, **62**, 358-368.

[20] Y. Xu, S. Zheng, H. Tang, X. Guo, H. Xue, H. Pang, *Energy Storage Mater.*, 2017, **9**, 11-30.

[21] J.-R. Jiménez, M. Tricoire, D. Garnier, L.-M. Chamoreau, J. von Bardeleben, Y. Journaux, Y. Li, R. Lescouëzec, *Dalton Trans.*, 2017, **46**, 15549-15557.

[22] S. F. Jafri, E. S. Koumousi, M.-A. Arrio, A. Juhin, D. Mitcov, M. Rouzières, P. Dechambenoit, D. Li, F. Otero, E. Wilhelm, A. Rogalev, L. Joly, J.-P. Kappler, C. Cartier dit Moulin, C. Mathonière, R. Clérac, P. Sainctavit, *J. Am. Chem. Soc.*, 2019, **141**, 3470-3479.

[23] V. Trannoy, A. Bordage, J. Dezalay, R. Saint-Martin, E. Rivière, P. Beaunier, C. Baumier, C. La Fontaine, G. Fornasieri, A. Bleuzen, *CrystEngComm*, 2019, **21**, 3634-3643.

[24] M.-A. Arrio, P. Sainctavit, C. Cartier dit Moulin, T. Mallah, M. Verdaguer, E. Pellegrin, C. Chen, *J. Am. Chem. Soc.*, 1996, **118**, 6422-6427.

[25] M. Giorgetti, M. Berrettoni, A. Filipponi, P. Kulesza, R. Marassi, *Chem. Phys. Lett.*, 1997, **275**, 108-112.

[26] T. Yokoyama, T. Ohta, O. Sato, K. Hashimoto, *Phys. Rev. B*, 1998, **58**, 8257-8266.

[27] A. Bleuzen, C. Lomenech, V. Escax, F. Villain, F. Varret, C. Cartier dit Moulin, M. Verdaguer, *J. Am. Chem. Soc.*, 2000, **122**, 6648-6652.

[28] V. Escax, A. Bleuzen, C. Cartier dit Moulin, F. Villain, A. Goujon, F. Varret, M. Verdaguer, *J. Am. Chem. Soc.*, 2001, **123**, 12536-12543.

[29] M. Giorgetti, M. Berrettoni, *Inorg. Chem.*, 2008, **47**, 6001-6008.

[30] S. Bonhommeau, N. Pontius, S. Cobo, L. Salmon, F. de Groot, G. Molnár, A. Bousseksou, H. Dürr, W. Eberhardt, *Phys. Chem. Chem. Phys.*, 2008, **10**, 5882-5889.

[31] T. Yokoyama, M. Kiguchi, T. Ohta, O. Sato, Y. Einaga, K. Hashimoto, *Phys. Rev. B*, 1999, **60**, 9340-9346.

[32] C. Cartier dit Moulin, F. Villain, A. Bleuzen, M.-A. Arrio, P. Sainctavit, C. Lomenech, V. Escax, F. Baudelet, E. Dartyge, J.-J. Gallet, M. Verdaguer, *J. Am. Chem. Soc.*, 2000, **122**, 6653-6658.

[33] A. Bleuzen, V. Escax, A. Ferrier, F. Villain, M. Verdaguer, P. Münsch, J.-P. Itié, *Angew. Chem. Int. Ed.*, 2004, **43**, 3728-3731.

[34] C. Cartier dit Moulin, G. Champion, J.-D. Cafun, M.-A. Arrio, A. Bleuzen, *Angew. Chem. Int. Ed.*, 2007, **46**, 1-4.

[35] J.-D. Cafun, G. Champion, M.-A. Arrio, C. Cartier dit Moulin, A. Bleuzen, *J. Am. Chem. Soc.*, 2010, **132**, 11552-11559.

[36] D. M. Pajerowski, B. Ravel, C. H. Li, M. F. Dumont, D. R. Talham, *Chem. Mater.*, 2014, **26**, 2586-2594.

[37] G. Fornasieri, A. Bordage, A. Bleuzen, *Eur. J. Inorg. Chem.*, 2018, **2018**, 259-271.

[38] A. Bordage, A. Bleuzen, *Radiat. Phys. Chem.*, 2020, **175**, article no. 108143.

[39] A. Bordage, R. Moulin, E. Fonda, G. Fornasieri, E. Rivière, A. Bleuzen, *J. Am. Chem. Soc.*, 2018, **140**, 10332-10343.

[40] P. Glatzel, U. Bergmann, *Coord. Chem. Rev.*, 2005, **249**, 65-95.

[41] P. Glatzel, L. Jacquamet, U. Bergmann, F. de Groot, S. P. Cramer, *Inorg. Chem.*, 2002, **41**, 3121-3127.

[42] G. Van der Laan, A. I. Figueroa, *Coord. Chem. Rev.*, 2014, **277–278**, 95-129.

[43] B. T. Thole, P. Carra, F. Sette, G. van der Laan, *Phys. Rev. Lett.*, 1992, **68**, 1943-1946.

[44] P. Carra, B. T. Thole, M. Altarelli, X. Wang, *Phys. Rev. Lett.*, 1993, **70**, 694-697.

[45] F. de Groot, A. Kotani, *Core Level Spectroscopy of Solids*, CRC Press, Taylor & Francis Group, Boca Raton, FL, 2008.

[46] M. L. Baker, Y. Kitagawa, T. Nakamura, K. Tazoe, Y. Narumi, Y. Kotani, F. Iijima, G. N. Newton, M. Okumura, H. Oshio, H. Nojiri, *Inorg. Chem.*, 2013, **52**, 13956-13962.

[47] Y. Prado, M.-A. Arrio, F. Volatron, E. Otero, C. Cartier dit Moulin, P. Sainctavit, L. Catala, T. Mallah, *Chem. Eur. J.*, 2013, **19**, 6685-6694.

[48] E. S. Koumousi, "Synthesis and characterization of dinuclear [Fe(μ-CN)Co] complexes exhibiting metal-to-metal electron transfer properties", PhD Thesis, Université de Bordeaux, 2015.

[49] S. F. Jafri, "Photomagnetic cobalt ferrycianide Prussian Blue Analogues probed by X-ray magnetic circular dichroism (XMCD)", PhD Thesis, Université Pierre et Marie Curie, 2016.

[50] S. F. Jafri, M.-A. Arrio, A. Bordage, R. Moulin, A. Juhin, C. Cartier dit Moulin, E. Otero, P. Ohresser, A. Bleuzen, P. Sainctavit, *Inorg. Chem.*, 2018, **57**, 7610-7619.

[51] G. Schütz, W. Wagner, W. Wilhelm, P. Kienle, R. Zeller, R. Frahm, G. Materlik, *Phys. Rev. Lett.*, 1987, **58**, 737-740.

[52] T. Funk, A. Deb, S. J. George, H. Wang, S. P. Cramer, *Coord. Chem. Rev.*, 2005, **249**, 3-30.

[53] A. Rogalev, F. Wilhelm, *Phys. Met. Metallogr.*, 2015, **116**, 1285-1336.

[54] A. Rogalev, K. Ollefs, F. Wilhelm, "X-ray magnetic circular dichroism", in *X-ray Absorption and X-ray Emission Spectroscopy—Theory and Applications (Volume II)* (J. A. van Bokhoven, C. Lamberti, eds.), Wiley, Hoboken, NJ, 2016, 671-694.

[55] R. Torchio, O. Mathon, S. Pascarelli, *Coord. Chem. Rev.*, 2014, **277–278**, 80-94.

[56] F. Baudelet, L. Nataf, R. Torchio, *High Pressure Res.*, 2016, **36**, 429-444.

[57] H. Ebert, P. Strange, B. Gyorffy, *J. Appl. Phys.*, 1988, **63**, 3055-3057.

[58] C. Brouder, M. Hikam, *Phys. Rev. B*, 1991, **43**, 3809-3820.

[59] J.-I. Igarashi, K. Hirai, *Phys. Rev. B*, 1994, **50**, 17820-17829.

[60] G. Guo, *J. Phys.: Condens. Matter*, 1996, **8**, L747-L752.

[61] G. Guo, *Phys. Rev. B*, 1998, **57**, 10295-10298.

[62] N. Bouldi, N. Vollmers, C. G. Delpy-Laplanche, Y. Joly, A. Juhin, P. Sainctavit, C. Brouder, M. Calandra, L. Paulatto, F. Mauri, U. Gerstmann, *Phys. Rev. B*, 2017, **96**, article no. 085123.

[63] N. Bouldi, P. Sainctavit, A. Juhin, L. Nataf, F. Baudelet, *Phys. Rev. B*, 2018, **98**, article no. 064430.

[64] V. Gadet, T. Mallah, I. Castro, M. Verdaguer, P. Veillet, *J. Am. Chem. Soc.*, 1992, **114**, 9213-9214.

[65] T. Mallah, S. Thiébaut, M. Verdaguer, P. Veillet, *Science*, 1993, **262**, 1554-1557.

[66] S. Ferlay, T. Mallah, R. Ouahès, P. Veillet, M. Verdaguer, *Nature*, 1995, **378**, 701-703.

[67] T. Mallah, S. Ferlay, C. Auberger, C. Hélary, F. L'Hermite, R. Ouahès, J. Vaissermann, M. Verdaguer, P. Veillet, *Mol. Cryst. Liq. Cryst.*, 1995, **273**, 141-151.

[68] M. Verdaguer, T. Mallah, C. Hélary, F. L'Hermite, P. Sainctavit, M.-A. Arrio, D. Babel, F. Baudelet, E. Dartyge, A. Fontaine, *Physica B*, 1995, **208–209**, 765-767.

[69] E. Dujardin, S. Ferlay, X. Phan, C. Desplanches, C. Cartier dit Moulin, P. Sainctavit, F. Baudelet, E. Dartyge, P. Veillet, M. Verdaguer, *J. Am. Chem. Soc.*, 1998, **120**, 11347-11352.

[70] J. M. Herrera, A. Bachschmidt, F. Villain, A. Bleuzen, V. Marvaud, W. Wernsdorfer, M. Verdaguer, *Phil. Trans. R. Soc. A*, 2008, **366**, 127-138.

[71] G. Champion, V. Escax, C. Cartier dit Moulin, A. Bleuzen, F. Villain, F. Baudelet, E. Dartyge, M. Verdaguer, *J. Am. Chem. Soc.*, 2001, **123**, 12544-12546.

[72] V. Escax, C. Cartier dit Moulin, F. Villain, G. Champion, J.-P. Itié, P. Münsch, M. Verdaguer, A. Bleuzen, *C. R. Chim.*, 2003, **6**, 1165-1173.

[73] A. Bleuzen, V. Escax, J.-P. Itié, P. Münsch, M. Verdaguer, *C. R. Chim.*, 2003, **6**, 343-352.

[74] O. Sato, Y. Einage, T. Iyoda, A. Fujishima, K. Hashimoto, *Science*, 1996, **272**, 704-705.

[75] V. Gadet, "Matériaux magnétiques moléculaires : du gap de Haldane à l'aimant", PhD Thesis, Université Paris VI, 1992.

[76] D. Lahiri, Y. Choi, S. M. Yusuf, A. Kumar, N. Ramanan, S. Chattopadhyay, D. Hashel, S. M. Sharma, *Mol. Cryst. Liq. Cryst.*, 1995, **273**, 141-151.

[77] F. Baudelet, Q. Kong, L. Nataf, J.-D. Cafun, A. Congedutti, A. Monza, S. Chagnot, J.-P. Itié, *High Pressure Res.*, 2011, **31**, 136-139.

[78] J.-D. Cafun, J. Lejeune, J.-P. Itié, F. Baudelet, A. Bleuzen, *J. Phys. Chem. C*, 2013, **117**, 19645-19655.

[79] A. Bordage, L. Nataf, F. Baudelet, A. Bleuzen, *J. Phys.: Conf. Ser.*, 2016, **712**, article no. 012109.

[80] A. N'Diaye, A. Bordage, L. Nataf, F. Baudelet, T. Moreno, A. Bleuzen, *J. Synchrotron Radiat.*, 2021, **8**, 1127-1136.

[81] A. N'Diaye, "XMCD au seuil K des métaux de transition et Analogues du Bleu de Prusse : une nouvelle approche pour la compréhension des signaux", PhD Thesis, Université Paris-Saclay, 2022.

[82] M. Sikora, A. Juhin, T.-C. Weng, P. Sainctavit, C. Detlefs, F. de Groot, P. Glatzel, *Phys. Rev. Lett.*, 2010, **105**, article no. 037202.

[83] M. Sikora, A. Juhin, G. Simon, M. Zajac, K. Biernacka, C. Kapusta, L. Morellon, M. Ibarra, P. Glatzel, *J. Appl. Phys.*, 2012, **111**, article no. 07E301.

[84] A. Juhin, A. López-Ortega, C. Sikora, M. Carvallo, M. Estrader, S. Estradé, F. Peiró, M. D. Baró, P. Sainctavit, P. Glatzel, J. Nogués, *Nanoscale*, 2014, **6**, 11911-11920.

[85] N. Daffé, M. Sikora, M. Rovezzi, N. Bouldi, V. Gavrilov, S. Neveu, F. Choueikani, P. Ohresser, V. Dupuis, D. Taverna, A. Gloter, M.-A. Arrio, P. Sainctavit, A. Juhin, *Adv. Mater. Interfaces*, 2017, **4**, article no. 1700599.

[86] A. Juhin, P. Sainctavit, K. Ollefs, M. Sikora, A. Filipponi, P. Glatzel, F. Wilhelm, A. Rogalev, *J. Phys.: Condens. Matter*, 2016, **28**, article no. 505202.

[87] N. Bouldi, "Theory of X-ray circular dichroism and application to materials under pressure", PhD Thesis, Sorbonne Université, 2017.